Decoherence in Josephson Qubits from Dielectric Loss

John M. Martinis,[1,*] K. B. Cooper,[1] R. McDermott,[1] Matthias Steffen,[1] Markus Ansmann,[1] K. D. Osborn,[2] K. Cicak,[2]
Seongshik Oh,[2] D. P. Pappas,[2] R. W. Simmonds,[2] and Clare C. Yu[3]

[1]*Department of Physics, University of California, Santa Barbara, California 93106, USA*
[2]*National Institute of Standards and Technology, 325 Broadway, Boulder, Colorado 80305-3328, USA*
[3]*Department of Physics and Astronomy, University of California, Irvine, California 92697, USA*

Dielectric loss from two-level states is shown to be a dominant decoherence source in superconducting quantum bits. Depending on the qubit design, dielectric loss from insulating materials or the tunnel junction can lead to short coherence times. We show that a variety of microwave and qubit measurements are well modeled by loss from resonant absorption of two-level defects. Our results demonstrate that this loss can be significantly reduced by using better dielectrics and fabricating junctions of small area $\lesssim$ 10 μm^2. With a redesigned phase qubit employing low-loss dielectrics, the energy relaxation rate has been improved by a factor of 20, opening up the possibility of multiqubit gates and algorithms.

Superconducting qubits are a promising candidate for the construction of a quantum computer [1]. Circuits work well, and experiments have demonstrated single qubit operations with reasonably long coherence times [2–6]. A recent experiment with phase qubits [7] has shown that the states of two qubits may be simultaneously measured, enabling full tomographic characterization of more complex gates [1]. Unfortunately, further progress in this system is hindered by short coherence times. Why is the coherence of phase qubits notably shorter than that of charge or flux qubits? Understanding this issue will aid progress in all superconducting qubits, as the identification of decoherence sources is crucial for continued improvements [8–10].

We report here a new decoherence mechanism, dielectric loss from two-level states (TLS). This loss is particularly important because of its surprisingly large magnitude; it can dominate all other sources of decoherence. We study the dielectric loss from bulk insulating materials as well as the tunnel barrier. A distinction is made between these two decoherence channels, even though their fundamental source is the same, because the losses manifest themselves differently.

This loss mechanism has been overlooked because it arises from a new class of decoherence: it is equivalent to dissipation from a fermionic bath [11], which gives qualitatively different behavior than the more familiar bosonic dissipation appropriate for photons or phonons. We present here several experimental measurements and a simple TLS model that provides a detailed description of this important phenomenon. Finally, by understanding this loss, we have obtained in a first-generation redesign of our phase qubit a 20-fold increase in coherence times, comparable to those of other successful devices.

Superconducting qubits are nonlinear microwave resonators formed by the Josephson inductance of a tunnel junction and its self-capacitance. Coherence is destroyed by loss and noise in these electrical elements. For capacitors, energy loss comes from dissipation in the insulator (with dielectric constant ϵ), which is conventionally described by the loss tangent $\tan\delta = \text{Im}\{\epsilon\}/\text{Re}\{\epsilon\}$. Small loss tangents $\delta \lesssim 10^{-5}$ are desired, with the number of coherent oscillations in the qubit given by $Q \sim 1/\delta$.

The loss tangent has generally been ignored because materials have been assumed to exhibit low loss at low temperatures. Indeed, we and others find that microwave loss is negligible for the crystalline substrates Si and Al$_2$O$_3$ [5,12]. However, crossover wiring in complex superconducting devices requires an insulating spacer that is typically made from amorphous SiO$_2$ deposited by chemical vapor deposition (CVD). In Fig. 1 we present data showing the loss tangent of a microwave driven LC oscillator formed by a superconducting inductor and a 300 nm thick CVD SiO$_2$ capacitor with $C \sim 5$ pF. Two small coupling capacitors connect the input and output ports. We measure the transmitted power as a function of frequency and drive amplitude in order to extract the loss tangent. At low temperature $T = 25$ mK $\ll \hbar\omega/k$, where $\omega/2\pi \sim 6$ GHz is the resonance frequency, we find that the loss varies strongly with drive amplitude and thus cannot be described as a conventional resistor (bosonic bath). The loss tangent is low at high amplitude, but scales inversely with the resonator voltage $\langle V^2 \rangle^{1/2}$ until it saturates at an intrinsic loss tangent $\delta_i \approx 5 \times 10^{-3}$. Similar to high drive powers, high temperatures give lower loss (data not shown).

Conventional measurements at high temperature or power suggest low dielectric loss in CVD SiO$_2$. However, superconducting qubits operate in the $T, V \to 0$ regime, where the intrinsic loss of SiO$_2$ is largest. Hence, great care must be taken when choosing insulating dielectrics in any qubit design in order to prevent short coherence times.

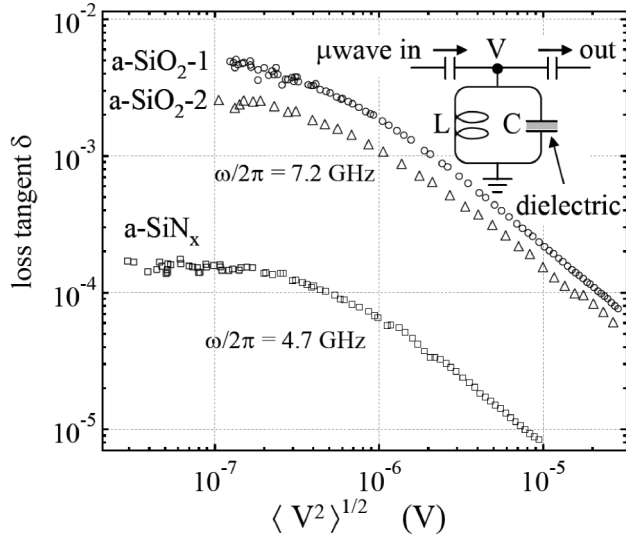Dielectric loss has been previously understood to arise from resonant absorption of microwave radiation by a bath

FIG. 1. Microwave dielectric loss for materials used in super-conducting qubit fabrication. The amorphous thin-film insulators were grown by chemical vapor deposition and form the dielectric of the resonator's parallel-plate capacitor. The a-SiO_2-1 (circles) and a-SiO_2-2 (triangles) data refer to amorphous SiO_2 deposited at $T = 13$ and $250\,°C$, respectively, using silane and oxygen as precursors. The a-SiN_x data refer to silicon nitride deposited at $T = 100\,°C$ by reacting silane and nitrogen.

of two-level systems possessing an electric dipole moment [13]. The power dependence of the loss arises from saturation of individual TLS, and for a parallel-plate geometry is given by

$$\delta = \frac{\pi \rho (ed)^2}{3\epsilon} \frac{\tanh(\hbar\omega/2kT)}{\sqrt{1 + \omega_R^2 T_1 T_2}}, \tag{1}$$

where x is the thickness, ρ is the TLS density of states each having a fluctuating dipole moment ed and relaxation times T_1 and T_2, and $\omega_R = (eVd/x)/\hbar$ is the TLS Rabi frequency. This theory fits our data well with parameters compatible with previous measurements of bulk SiO_2 [13].

Tunnel junctions are similarly made from amorphous dielectric materials; are they also lossy? A key difference is that tunnel junctions have small volume, and the assumption of a continuous distribution of defects is incorrect. Instead, dielectric loss must be described by a sparse bath of discrete defects. Individual defects can be measured spectroscopically with the phase qubit [14,15], and in Fig. 2(a) we plot the peak value of the occupation probability of the qubit $|1\rangle$ state as a function of excitation frequency and qubit bias. Along with the expected bias dependence, the data also exhibit avoided two-level crossings (splittings) that arise from the qubit state resonating with individual TLS in the tunnel barrier. These data demonstrate the qualitative trend that small-area qubits show fewer splittings than do large-area qubits, although larger splittings are observed in the smaller junctions. The presence of these spurious resonances can be quantified by
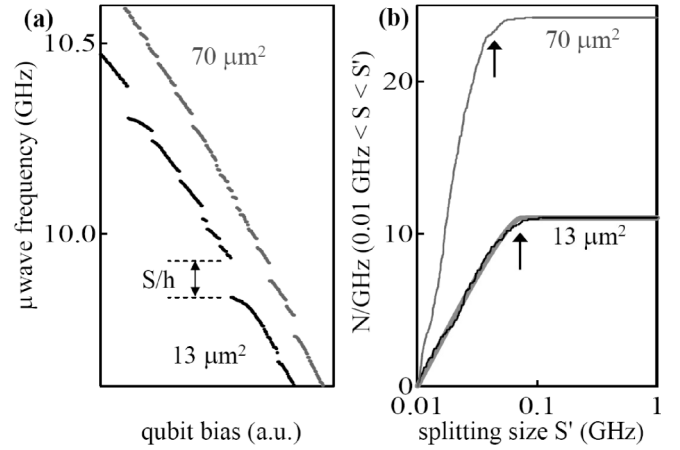

FIG. 2. Measurement of junction resonances and their size distribution. (a) Spectroscopy of the $0 \to 1$ qubit transition as a function of junction bias for two representative phase qubits with junction areas 13 μm^2 and 70 μm^2 (shifted for clarity). (b) Size distribution of splittings. The arrows indicate the cutoff $S_{\max}$.

measuring the amplitude S/h of each splitting, and then calculating the histogram of amplitudes. For clarity, this distribution is better analyzed through an integral of the number of splittings starting from the minimum experimental resolution of 0.01 GHz to S'/h and normalized to a 1 GHz bandwidth. The averages of the corresponding integrals for seven large-area qubits and four small-area qubits are shown in Fig. 2(b). When plotted versus $\log(S')$, we find the data fall on a line with an abrupt cutoff at $S_{\max}$, beyond which no further splittings are found. Furthermore, the slope of the line increases with qubit junction area A, and $S_{\max}$ decreases with increasing A.

Although the splittings were initially understood as arising from TLS fluctuations of the critical current [14], we now believe that charge fluctuations better describe the data [16]. In this model, the interaction Hamiltonian between a TLS and the qubit is given by $H_{\mathrm{int}} = (eVd/x) \times \cos\eta$, where η is the relative angle of the dipole moment ed with respect to the electric field V/x. For a single TLS dipole with two configurations L and R, the general Hamiltonian is $2H_{\mathrm{TLS}} = \Delta(|L\rangle\langle L| - |R\rangle\langle R|) + \Delta_0(|L\rangle\langle R| + |R\rangle\langle L|)$. The eigenstates $|g\rangle = \sin(\theta/2)|L\rangle - \cos(\theta/2)|R\rangle$ and $|e\rangle = \cos(\theta/2)|L\rangle + \sin(\theta/2)|R\rangle$ have a energy difference $E = \sqrt{\Delta^2 + \Delta_0^2}$, where $\tan\theta = \Delta_0/\Delta$. For a phase qubit with capacitance C and a transition energy E_{10} between states $|1\rangle$ and $|0\rangle$, the effective interaction Hamiltonian is $H_{\mathrm{int}} = i(S/2)(|1\rangle|g\rangle\langle 0|\langle e| - |0\rangle|e\rangle\langle 1|\langle g|)$ where S gives the size of the splitting on resonance:

$$S = S_{\max} \cos\eta \sin\theta, \tag{2}$$

$$S_{\max} = 2 \frac{d}{x} \sqrt{\frac{e^2}{2C} E_{10}}. \tag{3}$$

The expected distribution of the splitting sizes can be

calculated using the standard TLS tunneling model, where Δ is assumed to have a constant distribution and Δ_0 has a distribution proportional to $1/\Delta_0$ [17]. Changing the basis to more physical variables, the energy E and the dipole matrix element $\sin\theta$ [see Eq. (2)], one finds the state density $d^2N/dEd\sin\theta \propto 1/\sin\theta\cos\theta$. An average over η yields

$$\frac{d^2N}{dEdS} = \sigma A \frac{\sqrt{1 - S^2/S_{\max}^2}}{S} \qquad (4)$$

for $S < S_{\max}$ and 0 otherwise, where σ is a materials constant describing the defect density.

This prediction is consistent with the measured splitting distributions of Fig. 2(b), where the integrated density of splittings dN/dE increases as $\log S$ until reaching a cutoff at $S_{\max}$. In Fig. 2(b), the thick gray trace shows a good fit of the theory to the 13 μm^2 data using parameters $\sigma h = 0.5/\mu m^2\,GHz$ and $S_{\max}/h = 0.074$ GHz. Although the relative slope of the 70 μm^2 data scales slower than A, Monte Carlo simulations confirm this arises from large resonances overlapping smaller ones, shadowing their presence. The arrows, which indicate the fitted values of $S_{\max}$, agree with the scaling $1/\sqrt{A}$ predicted by Eq. (3). The measured $S_{\max}$, along with the qubit capacitance and resonant frequency, yield a dipole moment with $d/x \simeq 0.06$. This agrees with previous measurements [13,18,19] and makes physical sense since $d \simeq 0.13$ nm corresponds to a single charge moving a distance of a single atomic bond. This numerical agreement strongly suggests that these junction resonances arise from charge TLS and not critical-current fluctuations.

To calculate decoherence from the resonances, we first introduce a new quantity: the average number of resonances that couple to the qubit. An estimate of this number comes from counting the resonances that fall within a frequency $\pm S/2$ of the qubit frequency:

$$N_c = \int_0^{S_{\max}} \frac{d^2N}{dEdS} dS \int_{E_{10}-S/2}^{E_{10}+S/2} dE \qquad (5)$$

$$= (\pi/4)\sigma A S_{\max} \qquad (6)$$

$$= \sqrt{A/A_c}, \qquad (7)$$

where $A_c \simeq 90\ \mu m^2$ for AlO_x. Charge and flux qubits typically have $N_c \ll 1$, whereas for phase qubits $N_c \sim 1$.

For large-area junctions $N_c \gg 1$, the qubit couples to many junction resonances and the decay rate $|1\rangle \rightarrow |0\rangle$ may be calculated using the Fermi golden rule:

$$\Gamma_1 = \frac{2\pi}{\hbar} \int \frac{d^2N}{dEdS} (S/2)^2 dS \qquad (8)$$

$$= (\pi/6)\sigma A S_{\max}^2/\hbar \qquad (9)$$

$$= \frac{\pi(\sigma/x)(ed)^2}{3\epsilon} \frac{E_{10}}{\hbar}. \qquad (10)$$

This decay rate is equivalent to a dielectric loss tangent

$\delta_i = \hbar\Gamma_1/E_{10}$ and corresponds to the $T, V \rightarrow 0$ limit of Eq. (1).

Using Eq. (9) and the values of σ and $S_{\max}$ determined in Fig. 2, we calculate a decay time $1/\Gamma_1 = 8$ ns that agrees with the measured values 10–20 ns obtained for qubits with junction area 186 μm^2. The tunnel barrier loss tangent is large $\delta_i \simeq 1.6 \times 10^{-3}$, comparable to that of CVD SiO_2. This value is also reasonably consistent with a previous measurement of an AlO_x capacitor [20].

To understand decoherence for $N_c \lesssim 1$, we have performed Monte Carlo simulations of the interaction between the qubit and a collection of resonances randomly distributed according to Eq. (4). While the exact qubit dynamics depend upon the locations of the resonances, our simulations clearly show that the effects of dielectric loss may be statistically avoided by designing qubits with $N_c \lesssim 1$. With a junction bias that avoids resonances, decoherence is independent of time and the probability of decaying to the ground state has an average magnitude of $N_c^2/2$. Small decoherence is thus achieved by using small-area junctions or high-quality (small σ) dielectrics for the tunnel barrier. Note that despite the good results that are currently obtained in small-area superconducting qubits, the conclusion that the tunnel junctions are of high quality is incorrect. The junction dielectric is actually quite lossy, but due to the small volume it is possible to statistically avoid the discrete nature of the loss.

We believe the large loss tangent of CVD SiO_2 and AlO_x largely explains why only a few experiments have obtained long coherence times. For our phase qubits, junction loss plays a prominent role in limiting the coherence for the 186 μm^2 junction. For our 70 μm^2 device, loss from SiO_2 is comparable to that from the junction itself, leading to nonexponential decay of the qubit state. For our 13 μm^2 device, loss from SiO_2 dominates since it contributes $\sim 10\%$ to the qubit capacitance. The most successful experiments involving charge and flux qubits [3,4,21] have used small-area junctions *and* simple designs with no lossy dielectrics directly connected to the qubit junction, consistent with our observations. Given the generic need for wiring crossovers in advanced designs of a quantum computer, understanding dielectric loss is important for future success of all qubit technologies.

The defect density of TLS, as described by the loss tangent, determines the magnitude of decoherence. Is it possible to lower δ_i by improving materials?

We suggest that OH defects are the dominant source of the TLS in our amorphous CVD SiO_2 and AlO_x dielectrics. Previous experiments have measured the intrinsic loss in undoped and doped bulk quartz at 100 to 1000 ppm concentrations C_{OH}. The loss tangent was found to scale roughly as $\delta_i \simeq 3.0 \times 10^{-5} + 0.4\ C_{OH}$ [22]. The SiO_2 studied in this experiment was deposited with plasma enhanced CVD techniques using SiH_4 and O_2 as precursor gases. A large concentration of OH is expected for these films, on the order of a few atomic percent [23]. The loss tangents we measure correlate with C_{OH} determined from
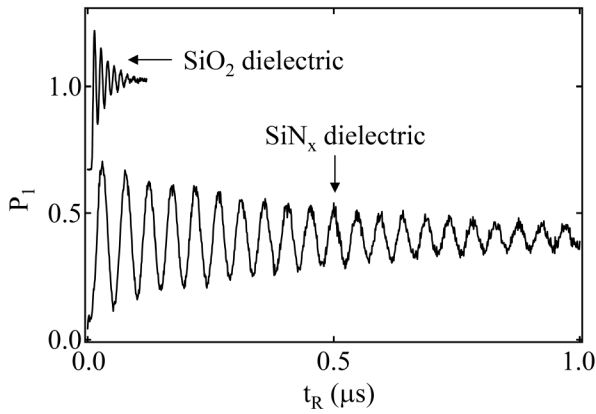
FIG. 3.   Rabi Oscillations for a phase qubit using CVD SiO_2 (top trace, offset) and SiN (bottom trace) as a dielectric for the crossover wiring. Microwaves at the qubit frequency are pulsed for a time t_R, and subsequent measurement of the qubit state shows an oscillation of the probability of the excited state. The decay of the Rabi oscillations is consistent with the measured relaxation time of $T_1 = 0.5$ μs, which is about 20 times better than previous experiments with a SiO_2 dielectric. From Ramsey fringes, we determined a dephasing time of $T_2 = 150$ ns (data not shown).

infrared spectroscopy and agrees in magnitude with an extrapolation of the bulk quartz data. We also note that a previous study measured C_{OH} in amorphous AlO_x to be as high as $2-8\%$ [24]; this suggests why the loss tangent of AlO_x is similar to that of CVD SiO_2.

In Fig. 1 we also show dielectric loss from CVD silicon nitride, made from precursor gases containing no oxygen. The intrinsic loss tangent was measured to be about 30 times smaller than for SiO_2, again confirming the importance of reducing the OH concentration

With SiN_x identified as a superior dielectric, the role of dielectric loss in phase qubits can be tested. In Fig. 3 we present Rabi oscillation data for two phase qubits, both with 13 μm^2 area but with different wiring designs. The top trace corresponds to our previous design with SiO_2 [15]. The bottom trace was obtained from a qubit with SiO_2 replaced with SiN_x and a reduction of the total amount of dielectric. The coherence time of the new device is about 20 times longer than previously attained, with Rabi oscillations still visible after 1 μs. This success gives compelling evidence that dielectric loss plays a major role in phase qubit decoherence and defines a clear direction for improvements in materials.

In conclusion, we have experimentally identified dielectric loss from two-level states as an important source of decoherence in superconducting qubits. Our results clearly point toward a need for a more in-depth understanding of

dissipation due to TLS because it *increases* as $T, V \to 0$, unlike conventional bosonic dissipation channels, and can hence lead to unexpected results. Given our observations, we are optimistic that new circuits and materials can be further developed to significantly improve the performance of all superconducting qubits.

*Electronic address: martinis@physics.ucsb.edu
[1] M. A. Nielsen and I. L. Chuang, *Quantum Computation and Quantum Information* (Cambridge University Press, Cambridge, 2000).
[2] Yu. A. Pashkin *et al.*, Nature (London) **421**, 823 (2003).
[3] D. Vion *et al.*, Science **296**, 886 (2002).
[4] I. Chiorescu *et al.*, Science **299**, 1869 (2003).
[5] A. Wallraff *et al.*, Nature (London) **431**, 162 (2004).
[6] J. M. Martinis *et al.*, Phys. Rev. Lett. **89**, 117901 (2002).
[7] R. McDermott *et al.*, Science **307**, 1299 (2005).
[8] P. Bertet *et al.*, cond-mat/0412485.
[9] E. Collin *et al.*, Phys. Rev. Lett. **93**, 157005 (2004).
[10] O. Astafiev *et al.*, Phys. Rev. Lett. **93**, 267007 (2004).
[11] A. Shnirman, G. Schön, I. Martin, and Y. Makhlin, Phys. Rev. Lett. **94**, 127002 (2005).
[12] P. K. Day *et al.*, Nature (London) **425**, 817 (2003).
[13] M. v. Schickfus and S. Hunklinger, Phys. Lett. A **64**, 144 (1977).
[14] R. W. Simmonds *et al.*, Phys. Rev. Lett. **93**, 077003 (2004).
[15] K. B. Cooper *et al.*, Phys. Rev. Lett. **93**, 180401 (2004).
[16] I. Martin, L. Bulaevskii, and A. Shnirman, Phys. Rev. Lett. **95**, 127002 (2005).
[17] S. Hunklinger and A. K. Raychaudhuri, Prog. Low Temp. Phys. **9**, 265 (1986); *Amorphous Solids: Low-Temperature Properties*, edited by W. A. Phillips (Springer, Berlin, 1981).
[18] B. Golding *et al.*, Phys. Rev. Lett. **43**, 1817 (1979).
[19] G. Baier and M. v. Schickfus, Phys. Rev. B **38**, 9952 (1988).
[20] I. Chiorescu *et al.*, Nature (London) **431**, 159 (2004).
[21] A. Wallraff *et al.*, Phys. Rev. Lett. **95**, 060501 (2005).
[22] M. v. Schickfus and S. Hunklinger, J. Phys. C **9**, L439 (1976).
[23] V. P. Tolstoy, I. Chernyshova, and V. A. Skryshevsky, *Handbook of Infrared Spectroscopy of Ultrathin Films* (Wiley-VCH, New York, 2003).
[24] J. Schneider *et al.*, Appl. Phys. Lett. **74**, 200 (1999).